RSC Advances

PAPER

View Article Online
View Journal | View Issue

Cite this: *RSC Adv.*, 2022, **12**, 27483

Insights into gold-catalyzed formation of aza-heterocycles using benzofuroxans as nitrene transfer reagents: mechanism and origins of chemoselectivity†

Weirong Wu, * Jiehui Liang, Biaolin Jiang, Xiaoxuan Tian and Tingzhen Li*

Received 27th August 2022
Accepted 20th September 2022

DOI: 10.1039/d2ra05382a

rsc.li/rsc-advances

Density functional theory (DFT) calculations have been performed to reveal the mechanism of gold(I)-catalyzed annulation of *N*-allylynamides and benzofuroxans as nitrene transfer reagents to construct azaheterocyclic compounds. The calculated results revealed that the reaction mechanism mainly undergoes eight processes. Among the reaction steps, intramolecular nucleophilic attack of the imino N atom on the α-position of activated gold keteniminium is a rate-determining process, which is different from that proposed previously by experiment. The chemoselectivity of the products is controlled by competition between the cyclopropanation of α-imino gold carbenes and intramolecular nucleophilic attack of the phenyl ring on α-imino gold carbenes, and could be explained by NPA charge. The different yields of cyclopropanated product in different solvents are dictated by the relative polarity leading to the different energy barriers of the rate-determining steps. The present work expounds the experimental observation at the molecular level and is informative for exploring efficient syntheses of 3-azabicyclo[3.1.0]hexanes.

1. Introduction

The cyclopropane core, a privileged motif in natural products and medicinal chemistry, has attracted tremendous attention ever since its discovery as it can serve as a versatile intermediate in organic reactions.[1] Among the methods established for preparing cyclopropanes,[2] gold-catalyzed reactions of nitrene transfer have been known as a promising methodology for the synthesis of bioactive miscellaneous aza-heterocyclic compounds.[3] Considerable effort has been devoted to developing transfer reagents, such as triazapentalene,[4] 2*H*-azirines,[5] azides,[6] isoxazole derivatives,[7] anthranils,[8] azirines,[9] pyridine-based aza-ylides[10] and sulfilimines,[11] to trap α-imino gold carbenes as key electrophilic intermediates *en route* to functional materials and aza-heterocycles (Scheme 1). Among these synthetic strategies for the generation of α-imino gold carbenes, unsatisfactorily, many nitrene transfer reagents exhibit substantial drawbacks, such as azides with potential explosivity and ylides with poor reactivity. Thus, the search for and use of new nitrene transfer reagents is highly challenging and desired as such α-imino gold carbenes can effectively be used to construct diversely functionalized carbo- or heterocycles.

Recently, benzofurazan *N*-oxides[12] have been considered as an effective and convenient nitrene transfer reagent for the generation of 2-amino-7-nitroindoles from ynamides due to its high reactivity, security, cheapness and accessibility.[13,14] However, compared with other nucleophilic nitrenes, *N*-oxides used as the precursors of α-imino gold-carbene intermediates for the cyclopropanation are less explored, especially in gold chemistry.

Excitingly, Dubovtsev's group[14] recently firstly reported a new approach for the generation of α-imino gold carbenes to construct 3-azabicyclo[3.1.0]hexanes *via* intramolecular cyclopropanation in highly selective gold-catalyzed annulations of *N*-allylynamides with benzofuroxans. In their representative one-pot reactions as indicated in Scheme 2, benzofuroxan **A1** is treated with *N*-allylynamide **A2** in the presence of $Ph_3PAuNTf_2$, the Gagosz catalyst, in chlorobenzene at 60 °C, leading to a 3-azabicyclo[3.1.0]hexane-2-imine **P1** as the major product in 92% isolated yield. A only trace amount of indole **P2** by CH insertion were detected. While the solvent chlorobenzene was replaced by acetonitrile, cyclopropanated product **P1** with a yield of 32% was observed.

A postulated reaction pathway for intramolecular cyclopropanation of gold α-imino carbenes generated from *N*-allylynamides and benzofuroxanes as nitrene transfer reagents was proposed by the Dubovtsev's group on the basis of their experimental observations (Scheme 3).

As for the uncommon reaction, although Dubovtsev's group proposed possible pathways, several important questions as to

School of Environment and Chemical Engineering, Chongqing Three Gorges University, Chongqing, China. E-mail: wuweirong011@163.com; litingzhen@163.com

† Electronic supplementary information (ESI) available. See https://doi.org/10.1039/d2ra05382a

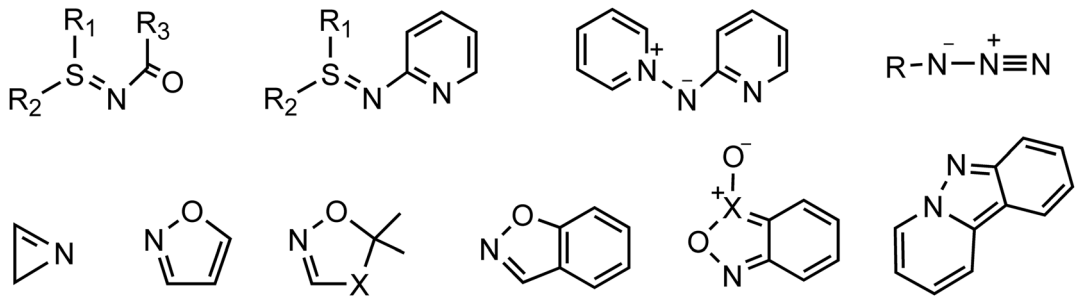

Scheme 1 Some nitrene transfer reagents.

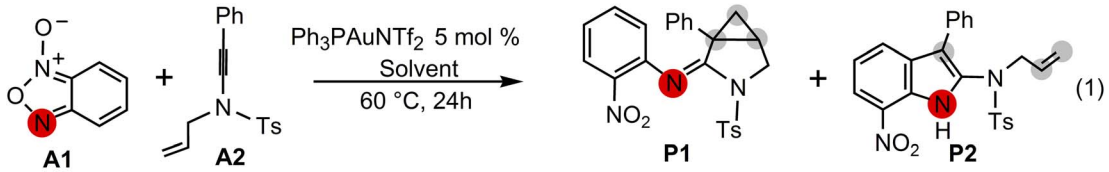

entry	Solvent	Yield(P1/P2)
1	PhCl	92%/trace
2	MeCN	32%/-

Scheme 2 Gold-catalyzed annulation of benzofuroxan **A1** with *N*-allylynamide **A2** reported by Dubovtsev's group.[14]

gold-catalyzed reaction of benzofuroxan **A1** with *N*-allylynamides **A2** *via* intramolecular cyclopropanation of gold α-imino carbene intermediates remains still unclear. For instance, what is the actual detailed mechanism and the chemoselectivity of products for the reactions in Scheme 2 ? An explicit picture for the reaction routs is highly desired. Which one is a key step of the catalytic reaction? What is the solvent effect in the light of previous reports[15,16]? Intrigued by α-imino gold carbenes and chemoselectivities, we here performed a systematic theoretical study to provide a better understanding of the intrinsic mechanism for prototypical reactions in this field. Interestingly, the calculated energetic details discovered the characteristics of the gold-catalyzed nitrene transfer from benzofuroxan to *N*-allylynamides for the synthesis of aza-heterocycles, expounding the experimental phenomenon at the molecular level. Our calculated results are expected to be informative for the development of a new strategy to access fused *N*-heterocyclic compounds using *N*-oxides used as the precursors of α-imino gold-carbene intermediates.

2. Computational details

The calculations were conducted with the Gaussian 09 package.[17] All structures were optimized at the B3LYP[18]/BSI level in the gas phase, BSI indicating a mixed basis set of the LANL2DZ[19] augmented with a f-type polarization function for

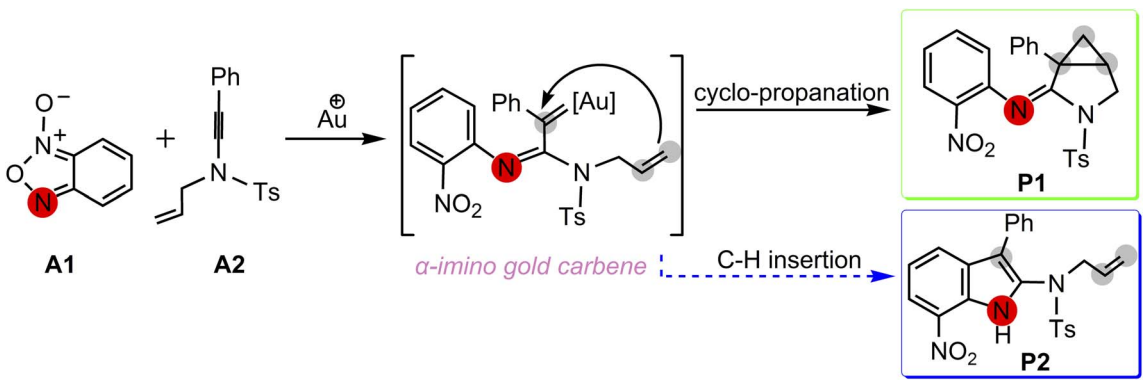

Scheme 3 Postulated pathways proposed by Dubovtsev's group[14] for the formation of 3-azabicyclo[3.1.0]hexane-2-imine **P1** *via* intramolecular cyclopropanation of the gold α-imino carbene intermediate.

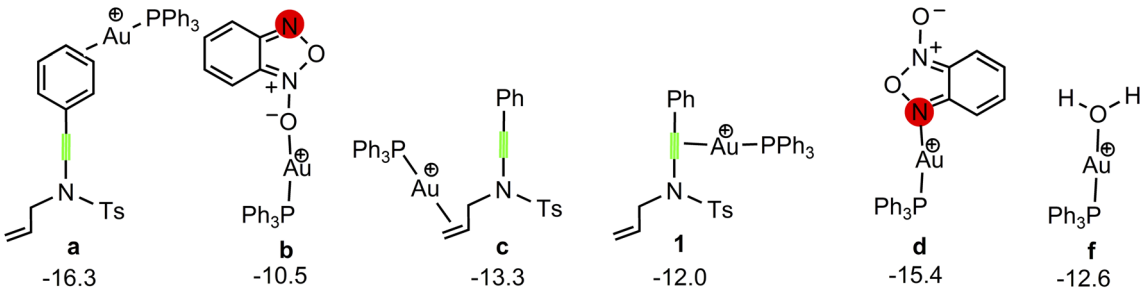

Scheme 4 Various potential coordinated gold(I) complex. The Gibbs free energies are given in kcal mol^{-1}.

Au, P and S atom and the 6–31g (d) for C, H, O and N atom. The orbital exponents used in calculation are H($\xi_P = 0.11$), O($\xi_d = 0.8$), N($\xi_d = 0.8$), P($\xi_d = 0.387$), C($\xi_d = 0.8$), S($\xi_d = 0.503$), and Au($\xi_f = 1.050$).[20] Frequency calculations for all reported structures at the same level of theory were carried out to confirm all the stationary points as energy ninima or transition states. Intrinsic reaction coordinate (IRC) analysis[21] was performed to confirm the connection of each transition state indeed with its forward and backward minima. To refine the calculated energies, we performed single-point free energy calculations using the solvation model density (SMD)[22] with a larger combined basis set. The SDD[23] (ECP) basis set is for Au, P and S, and the 6-311 + G(d, p) basis set for all the remaining atoms. Chlorobenzene and acetonitrile was used as the solvent with the UAKS atomic radii, in accordance with the experimental temperature. To reveal the detailed bonding feature, natural bond orbital (NBO) analyses were employed for the selected species.

3. Results and discussion

3.1 Formation of α-imino gold carbene intermediates

Our attention at first focuses on the reaction of benzofuroxan **A1** with *N*-allylynamide **A2** (eqn (1) in Scheme 2). To establish the most stable gold species, we investigated various potential coordinated complexes in the reaction system. All of the possible cationic PPh_3Au^+ adducts formed with H_2O molecular, substrates **A1** and **A2** are shown in Scheme 4. Clearly, adduct **a** is likely the resting state of the catalyst due to the fact that gold(I) complex is coordinated to the phenyl C=C π bond of *N*-allylynamide **A2** more strongly than other substrate. Fig. 1 shows the calculated formation pathways of α-imino gold carbene species.

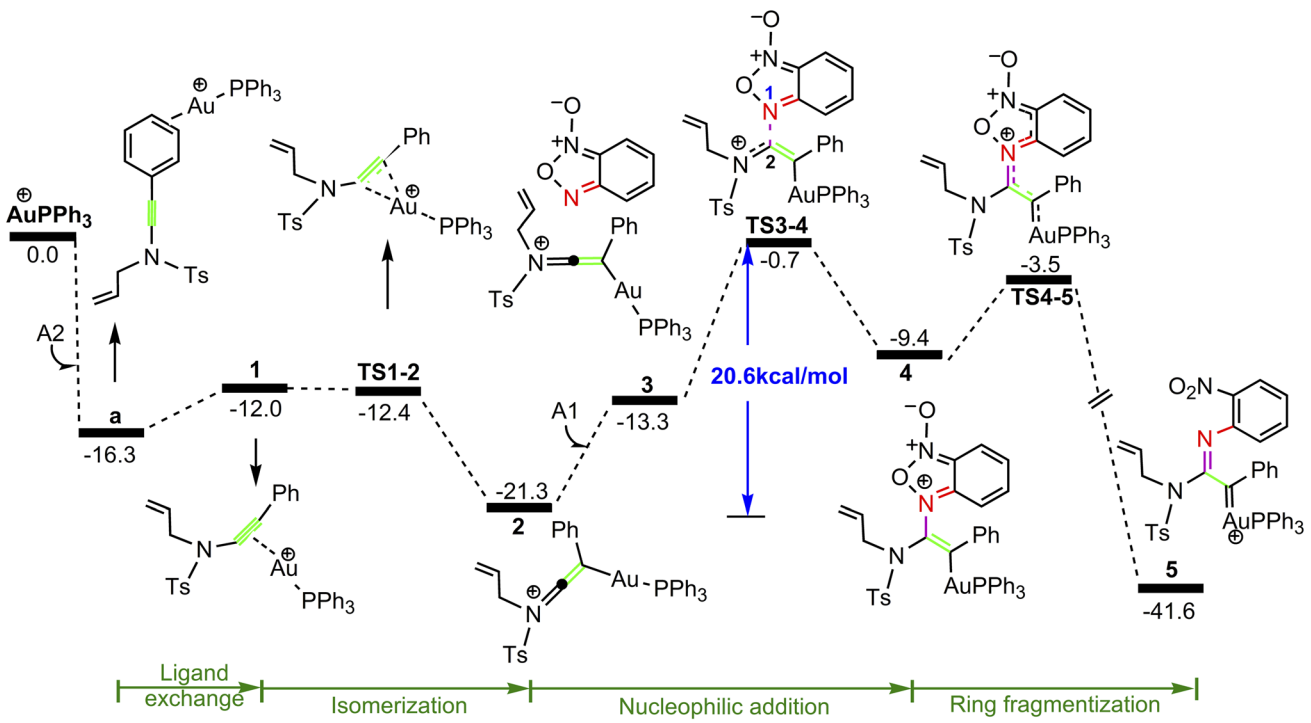

Fig. 1 Potential energy surface in PhCl solvent for the formation of gold α-imino carbene intermediate **5**. The Gibbs free energies are in kcal mol^{-1}.

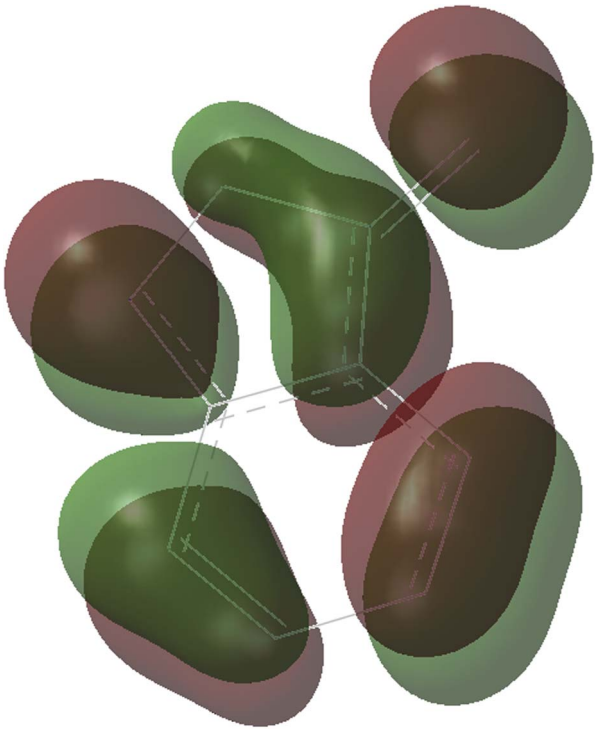

Fig. 2 The HOMO molecule orbital of benzofuroxan **A1**.

As shown in Fig. 1, the coordination of cationic PPh_3Au^+ species with phenyl C=C π bond of *N*-allylynamide **A2** affords initially a more stable gold(I) complex **a** as the resting state of the catalyst, releasing an energy of 16.3 kcal mol^{-1}. Subsequently, ligand exchange between alkynyl triple bond and phenyl C=C π bond of *N*-allylynamide **A2** takes place to give the alkyne-coordinated gold(I) complex **1**, from which isomerization process occurs *via* **TS1-2**, leading to the formation of a gold keteniminium species **2** without much of a kinetic barrier. This result implies that in agreement with previous proposals that interaction of gold complexes with electron-rich ynamides would facilely produce a electrophilic keteniminium species.[24] To facilitate subsequent nucleophilic attack, a unstable complex **3** relative to **2** is generated with the participating of benzofuroxan **A1**. In the following step, the reaction is surmised to proceed with nucleophilic attack of the imino N1 atom from the benzofuroxan **A1** on α-position of gold activated keteniminium species **2** to afford the vinyl-gold intermediate **4** *via* **TS3-4** with an overall barrier of 20.6 kcal mol^{-1} (the difference between **TS3-4** and **2**), and this process is identified as the rate-determining step for the catalytic reaction, which is different from that proposed by Dubovtsev's group.[14] In addition, we also considered the possibility of intramolecular attack by the O1 atom of N^+–O^- moiety instead of the imino N1 atom in **A1** on *in situ* generated ketenimine intermediate **2** to trigger generation of highly electrophilic α-oxo gold carbene intermediates. Unfortunately, the tying was failed, which is consistent with the

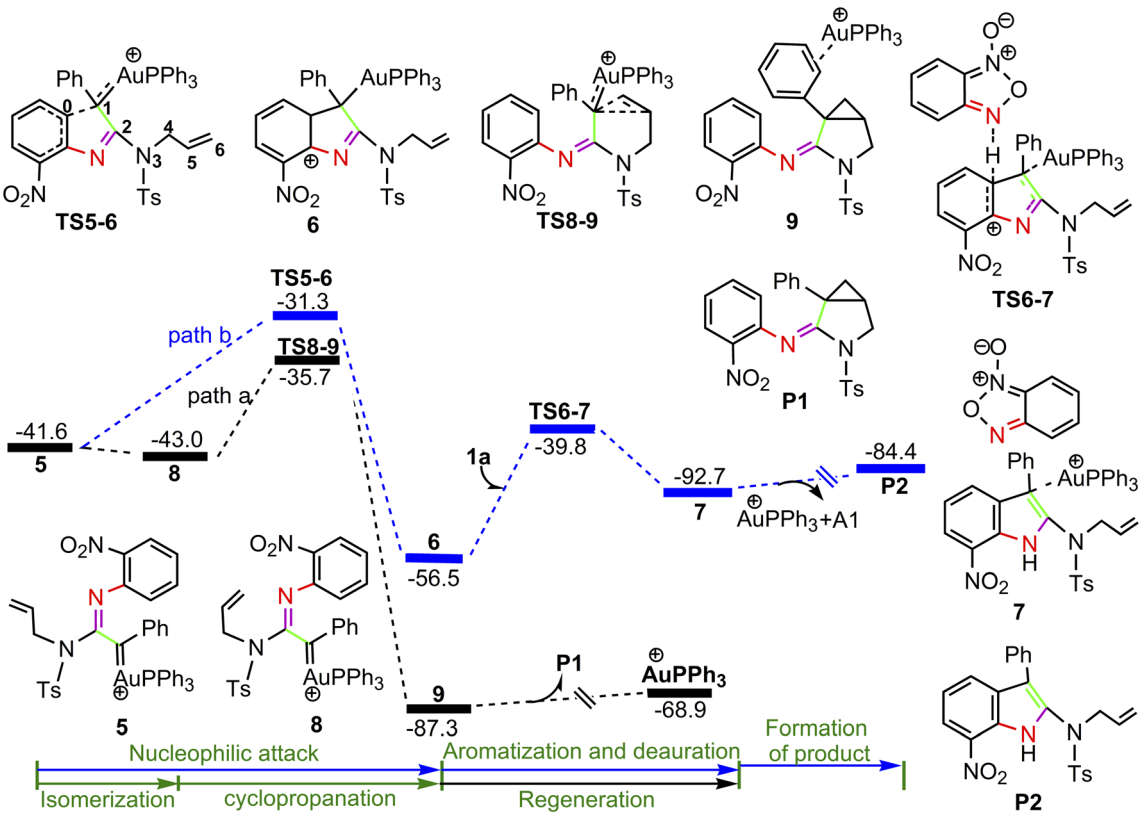

Fig. 3 Potential energy surface in PhCl solvent for the transformation of **5** to **P**. The solvent-corrected relative free energies are given in kcal mol^{-1}.

literature that the oxygen transfer reaction did not occur.[25] In nucleophilic reagent **A1**, obviously, the O1 atom of N^+–O^- moiety is much less reactive than the imino N1 atom in **A1** as a nucleophile. The fact can be rationalized by the highest occupied molecular orbital (HOMO) of **A1**. As shown in Fig. 2, electron density of the imino N1 atom is larger than that of the O1 atom of N^+–O^- moiety according to HOMO molecule orbital of **A1**. And the basicity of the imino N1 atom is stronger than the O1 atom of N^+–O^- moiety in **A1**. Henceforth, the reactivity of the imino N1 atom is better, which coincides with experimental observation[25] and previously theoretical calculation.[26] Next, ring fragmentization of **4** occurs to produce the reactive α-imino gold carbene **5**, a key intermediate. The low barrier (5.7 kcal-mol^{-1}) implies that this process is quite facile.

3.2 Formation of final product P from 5

The calculated profiles for the transformation of α-imino gold carbene intermediate **5** into cyclopropane product **P1** and indole **P2** are collected in Fig. 3. Once the gold α-imino carbene intermediate **5** is formed, there are two possibilities of nucleophilic attacks on gold carbenes and one possibility of cyclopropanation of gold carbenes (path a and b in Fig. 3, and path c in Fig. 4). In Fig. 3, path a starts from the rotation of the N3–C4–C5–C6 dihedral angle in **5** (D(N3C4C5C6) = −127.9°), leading to a slightly more stable isomer **8** (D(N3C4C5C6) = −3.4°) ready for subsequent intramolecular cyclopropanation. Then, concurrent additions of alkenyl C5 and C6 atoms to the gold carbene C1 atom take place *via* transition structure **TS8-9** with a low barrier of 7.3 kcal mol^{-1} to generate product-coordinated complex **9**. Finally, the desired product **P1** is gained along with release of cationic PPh_3Au^+ species. In contrast, intramolecular attack of the phenyl moiety on the Au-carbene C1 is relatively energy demanding with an activation barrier of 10.3 kcal mol^{-1} *via* transition structure **TS5-6** to generate a extremely unstable intermediate **6** over **8** by 30.8 kcal mol^{-1} (path b). The obvious free difference between **TS5-6** (31.3 kcal mol^{-1}) and **TS8-9** (35.7 kcal mol^{-1}) might be a result of de-aromatization transition state **TS5-6**. Subsequently, **6** would undergo aromatization by substrate **A1**-assisted H-shift with simultaneous deauration process to give complex **7**, the precursors of product **P2**, *via* transition state **TS6-7** with an activation barrier of 16.7 kcal mol^{-1}. The ensuing concomitant dissociation of **A1** molecule and cationic PPh_3Au^+ catalyst lead to the product **P2**.

For the path c of nucleophilic addition starting from **5** shown in Fig. 4, a isomerization process *via* **TS5-10** affords a slightly stable intermediate **10** by the slight rotation of C5═C6 π bond around C4–C5 bond in **5** (**5**: D(N3C4C5C6) = −127.9°, **10**: D(N3C4C5C6) = −129.8°). Subsequently, **10** would undergo intramolecular nucleophilic attack on the Au-carbene to give intermediate **11**. However, transition state **TS10-11** (−33.5 kcal mol^{-1}) has a higher free energy than **TS8-9**

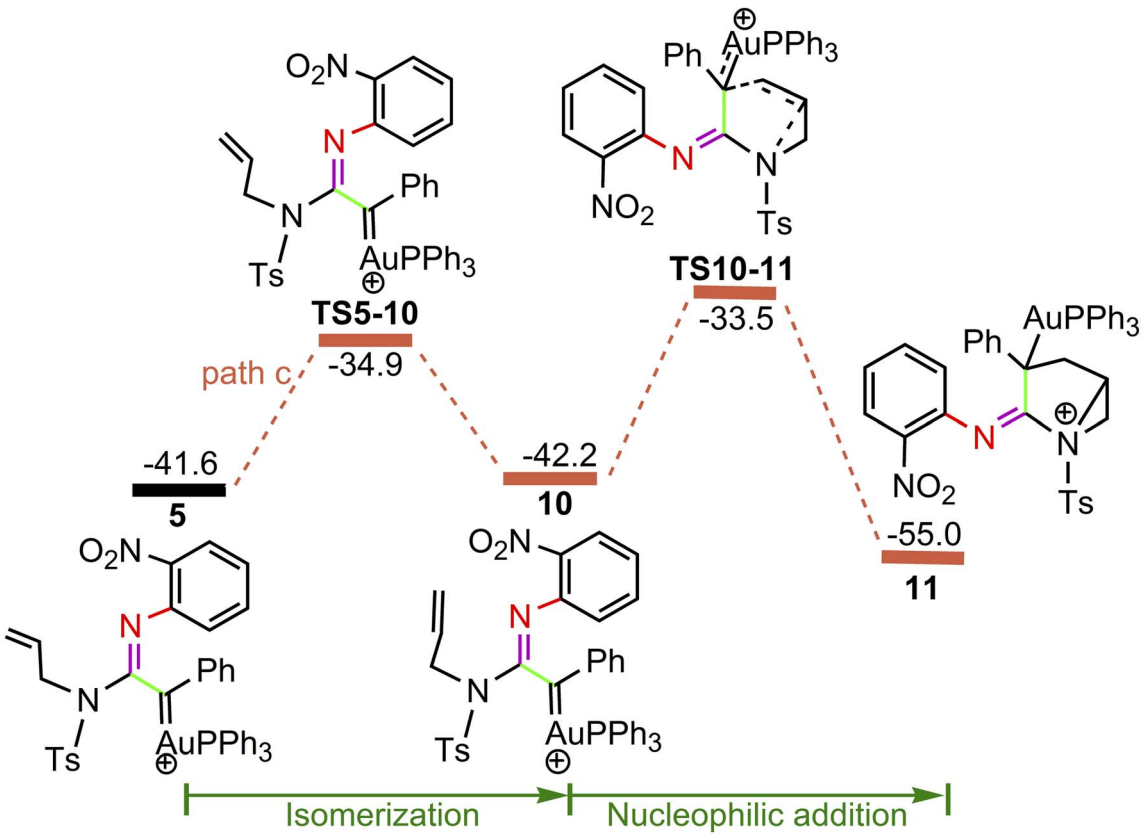

Fig. 4 Potential energy surface in PhCl solvent for the other pathway of nucleophilic attacks on α-imino gold carbene **5**. The solvent-corrected relative free energies are given in kcal mol^{-1}.

(-35.7 kcal mol^{-1}) in Fig. 3, which indicated that the pathway towards intermediate **11** would be unfavorable. Based on Fig. 1 and 3, it is clear that the key step of the whole catalytic cycle is intramolecular nucleophilic addition of the imino N1 atom to Au-carbene C1 *via* **TS3-4** (**2**→**3**→**TS3-4**→**4**) rather than intramolecular cyclopropanation of α-imino gold carbene intermediates as proposed previously by the experiments, and the overall barrier for this step is calculated to be as much as 20.6 kcal mol^{-1}, which is comparable with experimental conditions (60 °C), indicating that the pathway *via* the cyclopropanation of α-imino gold carbenes appears to be more favorable in the experimental condition (60 °C).

3.3 Origin of chemoselectivity

On the basis of the model reaction calculated (eqn (1) in Scheme 1), among the three pathways calculated, path a leading to the formation of cyclopropane product **P1** *via* **TS8-9** (-35.7 kcal mol^{-1}) is the most favourable pathway than path b towards indole **P2** *via* **TS5-6** (-31.3 kcal mol^{-1}) and path c *via* **TS10-11** (-33.5 kcal mol^{-1}) to give **11**. Experimentally, the reaction of benzofuroxan **A1** and *N*-allylynamide **A2** catalyzed by $Ph_3PAuNTf_2$ gave a 3-azabicyclo[3.1.0]hexane-2-imine **P1** (92% yield) and **P2** (trace). Clearly, **TS8-9** and **TS5-6** are the excellent chemodivergence-determining transition states towards two products (**P1** and **P2**). The overall barrier for **8**→**TS8-9** associated with the cyclopropanation of α-imino gold carbene **8**, another isomer of **5**, is lower by 3.0 kcal mol^{-1} in comparison to **5**→**TS5-6** related to intramolecular nucleophilic attack of the phenyl ring on gold carbene in **5**, explaining the experimentally observed results of the two products. The C–H insertion mechanism starting from **5** (path b) is unfavorable because the phenyl ring with the electron-withdrawing substituent (–NO_2 group) is not nucleophilic enough to make facilely the nucleophilic attack on the gold carbene, which might be corroborated by the NBO charge population analysis, the charge carried by phenyl C0 atom, and alkenyl C5 and C6 atoms in **5** are computed as $-0.259e$, $-0.242e$ and $-0.409e$, respectively.

3.4 Effect of solvent

Experiments showed that the yield of major product **P1** in acetonitrile (MeCN) decreases to 32%. It is obvious that solvent effects are involved in the reactivity of the catalytic reaction. In order to address this question, we calculated the relative free energy profiles towards **P1** and **P2** considering acetonitrile as the solvent. Fig. 5, S1 and S2† shows the potential energy surface in MeCN solvent for the reaction paths leading to **P1** and **P2**. As compared with the Gibbs energy profiles in PhCl, the obvious difference is the energy barrier of the rate-determining step (from **2** to **4**) of the whole catalytic cycle. For comparison, the calculated formation pathways of the α-imino gold carbene intermediate **5** in MeCN solvent are exhibited Fig. 5. Different form the situation in PhCl, the energy barrier calculated for nucleophilic attack by the imino nitrogen atom is 21.7 kcal mol^{-1} when MeCN is used as the solvent, higher than the overall barrier (20.6 kcal mol^{-1}) for the same process in PhCl, implying the nucleophilic addition is achievable and almost consistent with the experimental fact that the yield of **P1**

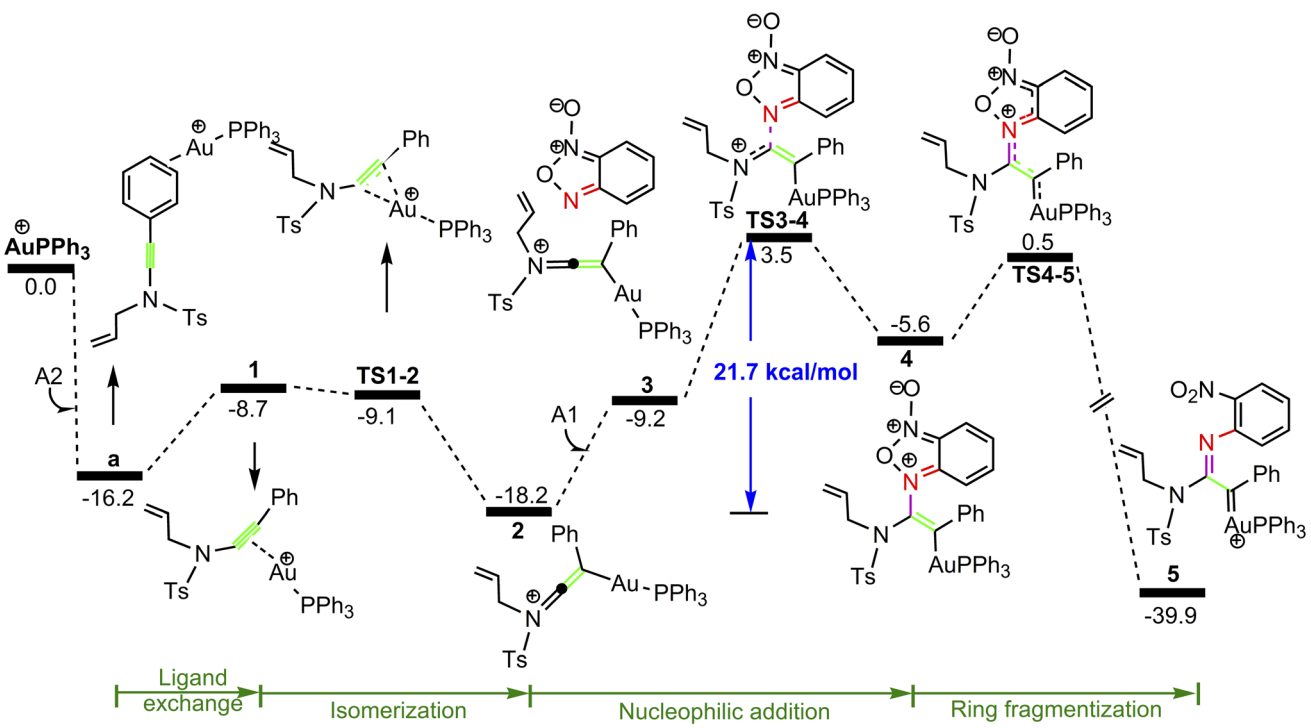

Fig. 5 Potential energy surface in MeCN solvent for the formation of the gold α-imino carbene intermediate **5**. The Gibbs free energies are in kcal mol^{-1}.

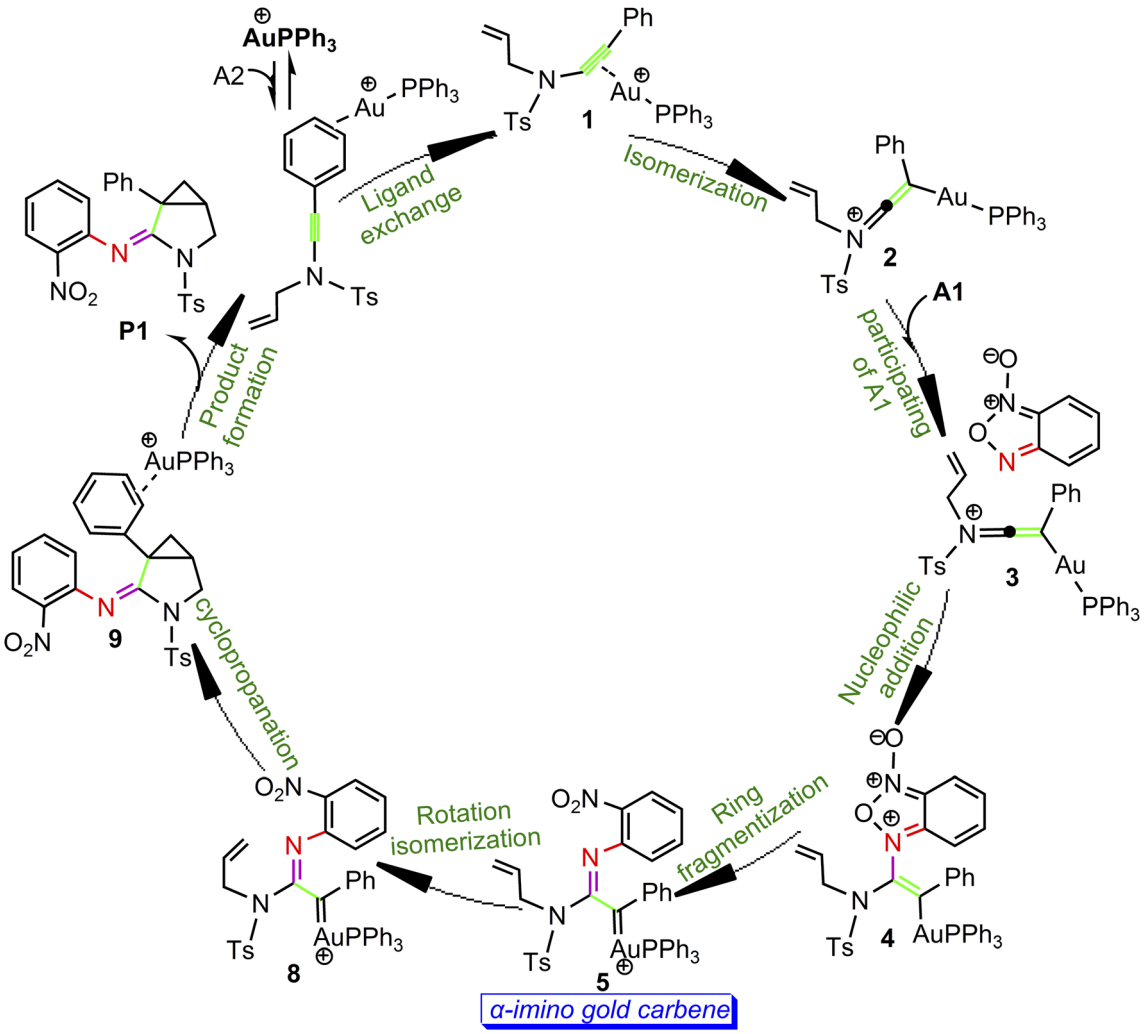

Scheme 5 Catalytic cycle derived from DFT calculations.

reached 32%. A plausible explanation for the solvent effects might be given as followed. As discussed above, almost all of the transition states and intermediates for the pathways are cationic species, and thus have relatively higher dipole moment. Clearly, the relative polarity of the **TS3-4** and **2** is the key factor leading to the different energy barriers of the rate-determining steps in the two solvents. The barrier differences $\Delta\Delta G = (\Delta G(\mathbf{TS3\text{-}4}) - \Delta G(\mathbf{2}))$ calculated in the PhCl and MeCN are 20.6 and 21.7 kcal mol^{-1}, respectively, indicating that the energy gap increases when the polarity of the solvent used increases. As a result, the strong polarity of MeCN as a solvent influences **TS3-4** and **2** more strongly than those in PhCl, resulting in the decrease of **P1** yield.

3.5 Proposed mechanism based on calculation

According to the above calculation results, the gold-catalyzed annulation of benzofuroxan **A1** as nitrene transfer reagents with *N*-allylynamide **A2** are summarized schematically in Scheme 5. In this catalytic reaction, complex **a** is predicted to be the catalytic resting state due to the fact that gold(I) complex is coordinated to the phenyl C=C π bond of *N*-allylynamide **A2** more strongly than other substrate. Ligand exchange between phenyl C=C π bond and alkyne occurs to give a alkyne-coordinated species **1**. The activation of *N*-allylynamide with Au(I) catalyst subsequently generates a highly electrophilic keteniminium intermediate **2**. With the participating of benzofuroxan **A1**, a unstable complex **3** relative to **2** is generated. Next, the nucleophilic attack of the imino N1 atom in benzofuroxan **A1** to α-position of activated gold keteniminium **2** to produce vinyl-gold intermediate **4**. The formation of α-imino gold carbene intermediate **5**, a key intermediate, occurs with ring fragmentization. Subsequent isomerization of **5** by the rotation of alkenyl C=C bond afford α-imino Au-carbene intermediate **8**. Finally, **8** undergoes the cyclopropanation process to give the desired product 3-azabicyclo[3.1.0]hexane-2-imine **P1**. According to our calculations, the transformation **2** + **A2** → **4** with an overall activation energy of 20.6 kcal mol^{-1} is the rate-determining step, completely different from that proposed by Dubovtsev's group.

4. Conclusion

The detailed mechanisms of the gold(I)-catalyzed annulation of benzofuroxan **A1** with *N*-allylynamide **A2** have been investigated with the aid of DFT calculations. The reaction pathways calculated mainly involve eight processes: ligand exchange between phenyl C=C π bond and alkyne, *N*-allylynamide activation to produce gold keteniminium species (isomerization), participating of benzofuroxan **A1**, intramolecular nucleophilic addition of imino N atom to α-position of the activated gold keteniminium, ring fragmentization of the vinyl-gold intermediate, isomerization by the rotation of alkenyl C=C bond, and cyclopropanation of the α-imino gold carbene leading to product formation. The chemoselectivity is controlled by competition of the cyclopropanation of α-imino gold carbenes and the nucleophilic attack of the phenyl ring on α-imino gold carbenes. The key step of the whole catalytic cycle is intramolecular nucleophilic addition of the imino N1 atom to Au-carbene C1 rather than intramolecular cyclopropanation of α-imino gold carbene complexes as proposed previously by the experiments, and the overall barrier for this step is calculated to be as much as 20.6 kcal mol^{-1}. The solvent effects could be revealed by the relative polarity leading to the different energy barriers of the rate-determining steps.

Conflicts of interest

The authors declare no competing financial interest.

References

1 (*a*) R. J. Breckenridge and C. J. Suckling, *Tetrahedron*, 1986, **42**, 5665; (*b*) S. Patai and Z. Rappoport, *The Chemistry of the Cyclopropyl Group*, John Wiley and Sons, New York, 1987; (*c*) J. Salaün, *Chem. Rev.*, 1989, **89**, 1247; (*d*) A. de Meijere, *Small Ring Compounds in Organic Synthesis VI*, Springer, Berlin, Germany, 2000; (*e*) J. Salaün, *Top. Curr. Chem.*, 2000, **207**, 1; (*f*) J. Pietruszka, *Chem. Rev.*, 2003, **103**, 1051; (*g*) B.-L. Lu, L. Dai and M. Shi, *Chem. Soc. Rev.*, 2012, **41**, 3318.

2 (*a*) W. A. Donaldson, *Tetrahedron*, 2001, **57**, 8589; (*b*) L. A. Wessjohann, W. Brandt and T. Thiemann, *Chem. Rev.*, 2003, **103**, 1625; (*c*) D. Y.-K. Chen, R. H. Pouwer and J.-A. Richard, *Chem. Soc. Rev.*, 2012, **41**, 4631.

3 (*a*) L.-W. Ye, X.-Q. Zhu, R. L. Sahani, Y. Xu, P.-C. Qian and R.-S. Liu, *Chem. Rev.*, 2021, **121**(14), 9039; (*b*) E. Aguilar and J. Santamaría, *Org. Chem. Front.*, 2019, **6**(9), 1513; (*c*) X. Zhao, M. Rudolph, A. M. Asiri and A. S. K. Hashmi, *Front. Chem. Sci. Eng.*, 2020, **14**(3), 317; (*d*) P. W. Davies and M. Garzón, *Asian J. Org. Chem.*, 2015, **4**(8), 694.

4 J. Gonzalez, J. Santamaría, A. L. Suarez-Sobrino and A. Ballesteros, *Adv. Synth. Catal.*, 2016, **358**, 1398.

5 (*a*) L. Zhu, Y. Yu, Z. Mao and X. Huang, *Org. Lett.*, 2015, **17**, 30; (*b*) A. Prechter, G. Henrion, P. F. dit Bel and F. Gagosz, *Angew. Chem. Int. Ed.*, 2014, **53**, 4959; *Angew. Chem.*, 2014, **126**, 5059; (*c*) S. K. Pawar, R. L. Sahani and R. S. Liu, *Chem.–Eur. J.*, 2015, **21**, 10843.

6 (*a*) D. J. Gorin, N. R. Davis and F. D. Toste, *J. Am. Chem. Soc.*, 2005, **127**, 11260; (*b*) B. Lu, Y. Luo, L. Liu, L. Ye, Y. Wang and L. Zhang, *Angew. Chem. Int. Ed.*, 2011, **50**, 8358; *Angew. Chem.*, 2011, **123**, 8508; (*c*) A. Wetzel and F. Gagosz, *Angew. Chem. Int. Ed.*, 2011, **50**, 7354; *Angew. Chem.*, 2011, **123**, 7492; (*d*) Y. Xiao and L. Zhang, *Org. Lett.*, 2012, **14**, 4662; (*e*) Z. Y. Yan, Y. Xiao and L. Zhang, *Angew. Chem. Int. Ed.*, 2012, **51**, 8624; *Angew. Chem.*, 2012, **124**, 8752; (*f*) Y. Tokimizu, S. Oishi, N. Fujii and H. Ohno, *Org. Lett.*, 2014, **16**, 3138; (*g*) C. Shu, Y.-H. Wang, B. Zhou, X.-L. Li, Y.-F. Ping, X. Lu and L.-W. Ye, *J. Am. Chem. Soc.*, 2015, **137**, 9567; (*h*) Y. Wu, L. Zhu, Y. Yu, X. Luo and X. Huang, *J. Org. Chem.*, 2015, **80**, 11407.

7 (*a*) A.-H. Zhou, Q. He, C. Shu, Y.-F. Yu, S. Liu, T. Zhao, W. Zhang, X. Lu and L.-W. Ye, *Chem. Sci.*, 2015, **6**, 1265; (*b*) H. Jin, L. Huang, J. Xie, M. Rudolph, F. Rominger and A. S. K. Hashmi, *Angew. Chem. Int. Ed.*, 2016, **55**, 794; *Angew. Chem.*, 2016, **128**, 804; (*c*) M. Chen, N. Sun, H. Chen and Y. Liu, *Chem. Commun.*, 2016, **52**, 6324; (*d*) H. Jin, B. Tian, X. Song, J. Xie, M. Rudolph, F. Rominger and A. S. K. Hashmi, *Angew. Chem. Int. Ed.*, 2016, **55**, 12688; *Angew. Chem.*, 2016, **128**, 12880; (*e*) R. L. Sahani and R.-S. Liu, *Angew. Chem. Int. Ed.*, 2017, **56**, 1026; *Angew. Chem.*, 2017, **129**, 1046; (*f*) Z. Zeng, H. Jin, J. Xie, B. Tian, M. Rudolph, F. Rominger and A. S. K. Hashmi, *Org. Lett.*, 2017, **19**, 1020; (*g*) Z. Zeng, H. Jin, K. Sekine, M. Rudolph, F. Rominger and A. S. K. Hashmi, *Angew. Chem. Int. Ed.*, 2018, **57**, 6935; *Angew. Chem.*, 2018, **130**, 7051.

8 Y. Wu, C. Hu, T. Wang, L. Eberle and A. S. K. Hashmi, *Adv. Synth. Catal.*, 2022, **364**, 1233.

9 N. V. Shcherbakov, G. D. Titov, E. I. Chikunova, I. P. Filippov, N. V. Rostovskii, V. Yu. Kukushkin and A. Yu. Dubovtsev, *Org. Chem. Front.*, 2022, DOI: **10.1039/D2QO01105K**.

10 (*a*) P. W. Davies, A. Cremonesi and L. Dumitrescu, *Angew. Chem. Int. Ed.Angew. Chem.*, 20112011, **50123**, 89319093; (*b*) C. Li and L. Zhang, *Org. Lett.*, 2011, **13**, 1738; (*c*) M. Garzln and P. W. Davies, *Org. Lett.*, 2014, **16**, 4850; (*d*) R. J. Reddy, M. P. Ball-Jones and P. W. Davies, *Angew. Chem. Int. Ed.*, 2017, **56**, 13310; *Angew. Chem.*, 2017, **129**, 13495; (*e*) E. Chatzopoulou and P. W. Davies, *Chem. Commun.*, 2013, **49**, 8617; (*f*) H.-H. Hung, Y.-C. Liao and R.-S. Liu, *Adv. Synth. Catal.*, 2013, **355**, 1545.

11 (*a*) X. Tian, L. Song, M. Rudolph, F. Rominger and A. S. K. Hashmi, *Org. Lett.*, 2019, **21**, 4327; (*b*) X. Tian, L. Song, M. Rudolph, F. Rominger, T. Oeser and A. S. K. Hashmi, *Angew. Chem., Int. Ed.*, 2019, **58**, 3589.

12 Z. Zheng, X. Ma, X. Cheng, K. Zhao, K. Gutman, T. Li and L. Zhang, *Chem. Rev.*, 2021, **121**(14), 8979.

13 W. Xu, Y. Chen, A. Wang and Y. Liu, *Org. Lett.*, 2019, **21**(18), 7613.

14 N. V. Shcherbakov, D. V. Dar'in, V. Y. Kukushkin and A. Y. Dubovtsev, *J. Org. Chem.*, 2021, **86**, 12964.

15 (*a*) N. V. Shcherbakov, D. V. Dar'in, V. Yu. Kukushkin and A. Yu. Dubovtsev, *J. Org. Chem.*, 2021, **86**(10), 7218; (*b*) A. Yu. Dubovtsev, V. V. Zvereva, N. V. Shcherbakov, D. V. Dar'in, A. S. Novikov and V. Yu. Kukushkin, *Org. Biomol. Chem.*, 2021, **19**, 4577; (*c*) N. V. Shcherbakov,

E. I. Chikunova, D. Dar'in, V. Yu. Kukushkin and A. Yu. Dubovtsev, *J. Org. Chem.*, 2021, **86**, 17804.

16 (*a*) M. Kumar, G. B. Hammond and B. Xu, *Org. Lett.*, 2014, **16**(13), 3452; (*b*) E. I. Chikunova, V. Yu. Kukushkin and A. Yu. Dubovtsev, *Green Chem.*, 2022, **24**, 3314.

17 M. J. Frisch, G. W. Trucks, H. B. Schlegel, G. E. Scuseria, M. A. Robb, J. R. Cheeseman, G. Scalmani, V. Barone, B. Mennucci, G. A. Petersson, *et al.*, *Gaussian 09, Revision A.02*, Gaussian, Inc., Wallingford, CT, 2009.

18 (*a*) Y. Zhao, N. E. Schultz and D. G. Truhlar, *J. Chem. Phys.*, 2005, **123**, 161103; (*b*) Y. Zhao and D. G. Truhlar, *Acc. Chem. Res.*, 2008, **41**, 157.

19 P. C. Hariharan and J. A. Pople, *Theor. Chim. Acta*, 1973, **28**, 213.

20 A. W. Ehlers, M. Bohme, S. Dapprich, A. Gobbi, A. Hollwarth, V. Jonas, K. F. Kohler, R. Stegmann, A. Veldkamp and G. Frenking, *Chem. Phys. Lett.*, 1993, **208**, 111.

21 (*a*) K. Fukui, *J. Phys. Chem.*, 1970, **74**, 4161; (*b*) K. Fukui, *Acc. Chem. Res.*, 1981, **14**, 363.

22 A. V. Marenich, C. J. Cramer and D. G. Truhlar, *J. Phys. Chem. B*, 2009, **113**, 6378.

23 P. Fuentealba, H. Stoll, L. Szentpaly, P. Schwerdtfeger and H. Preuss, *J. Phys. B: At. Mol. Phys.*, 1983, **16**, L323.

24 S. Shandilya, M. P. Gogoi, S. Dutta and A. K. Sahoo, *Chem. Rec.*, 2021, **21**, 4123.

25 W. Xu, Y. Chen, A. Wang and Y. Liu, *Org. Lett.*, 2019, **21**, 7613.

26 F. Zarkoob and A. Ariafard, *Organometallics*, 2019, **38**, 489.